PROPERTIES OF POROUS ANODIC ALUMINUM OXIDE FILMS AS MEMBRANES

KINGO ITAYA, SHIZUO SUGAWARA, KUNIO ARAI AND SHOZABURO SAITO

Department of Chemical Engineering, Tohoku University, Sendai 980

Key Words: Inorganic Membrane, Anodic Alumina Membrane, Ultrafiltration, Gas Permeability, Knudsen Flow

The details of a method of preparing anodic aluminum oxide membranes are presented. The porous oxide layer consists of close-packed cells of oxide, hexagonal in shape, each of which contains a single pore formed perpendicularly to the surface of the aluminum substrate. This special structural feature is essentially important for ultrafiltration and gas separation. The rejection characteristics are examined, using aqueous and nonaqueous solutions of macromolecules. The permeability of gases is also examined at different temperatures. The flow of gases is explained by the Knudsen regime alone.

Introduction

Membrane technology is now receiving a great deal of attention in membrane-based industries.[19] Membranes can be applied in microfiltration, ultrafiltration, dialysis, electrodialysis, reverse osmosis and gas separation, depending on the size of the pore and the nature of the material. Regarding the material of the membrane, organic polymer films have been extensively investigated. However, little attention has been paid to the development of inorganic materials as membranes. A semi-permeable membrane of cupric ferrocyanide was historically used for the direct determination of osmotic pressure.[9] Hydrous oxide membranes formed dynamically on porous bodies have been examined.[28] One of the most interesting examples of inorganic membranes seems to be a porous glass known under the brand-name of Vycor. Studies on this material have been reported for reverse osmosis[1,4,6] and gas separation.[12,13,27] One of the remarkable properties of the glass membrane is its stability at high temperatures. The application of this type of membrane has recently been the object of great interest in the field of gas separation, because of its importance in coal gas industries where CO and H_2 are primarily used. Porous silica and alumina membranes prepared by compaction of the powders have also been examined for gas separation.[10]

Against this background, we have investigated porous anodic aluminum oxide films for both ultrafiltration and gas separation. It is well known that porous anodic films can be formed on aluminum by anodizing in acid electrolytes such as sulfuric acid, oxalic acid, and phosphoric acid.[8] The structure of the porous anodic oxide film has been proposed by Keller *et al.*[17] and other groups.[20,22] As shown in **Fig. 1**, the anodic oxide film on aluminum consists of two regions, the so-called porous layer and the barrier layer. The porous layer consists of close-packed cells of oxide, predominantly hexagonal in shape, each of which contains a single pore formed perpendicularly to the macroscopic surface of the aluminum substrate. The barrier layer is a thin compact inner region lying adjacent to the metal. The pore diameters have been reported as ca. 10 nm, 20 nm and 30 nm for films prepared in sulfuric acid, oxalic acid and phosphoric acid, respectively.[8] This indicates that the pore diameter is primarily dependent on the electrolyte used.

Such films have previously come under investigation by Smith for dialysis membranes.[29] The osmotic flow of water and the counter flow of salt have been measured in the absence of external pressure. Porous anodic aluminum membranes have the advantage of high thermal stability and special structural features for ultrafiltration and gas separation, but, to our knowledge, have not previously been described.

In this paper, the details of a preparation method of preparing the membranes and the permeabilities of gases and solutes are discussed.

1. Experimental

1.1 Preparation of membrane

A 99.99% aluminum plate (thickness, 0.1–0.3 mm) was placed at ca. 10^7 Pa in order to obtain a flat substrate and then fully annealed for one hour at

Received March 9, 1984. Correspondence concerning this article should be addressed to S. Saito.

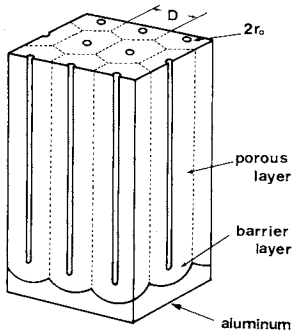

Fig. 1. Structure of anodic aluminum oxide. Dimensions of pore ($2r_0$) and cell (D) are indicated.

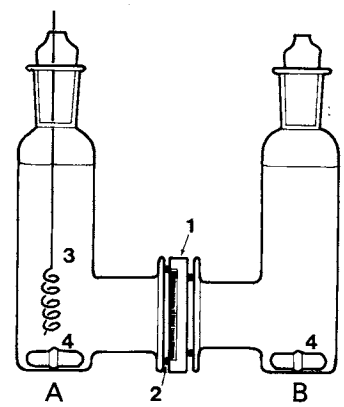

Fig. 2. Cell used for anodization of aluminum. 1) aluminum substrate; 2) o-rings; 3) platinum cathode; 4) stirring bars.

350°C in air. The plates were then degreased in acetone, washed in distilled water and chemically and electrochemically polished in chromic acids. After polishing, the plates were washed with water, dipped in a chromic acid solution (CrO_3; 45 g/l, H_3PO_4; 3.5% in volume) for a few minutes at 90°C to de-smudge, washed with water and dried.

Figure 2 shows the cell used for anodizing. Only one face of the substrate was anodized. Sulfuric acid (20 wt%) and oxalic acid (4 wt%) were mainly used as the electrolytes in order to obtain a fairly thick film. Because the formed oxide layer is etched slowly by sulfuric acids, the diameter of the pore will be widened by chemical dissolution.[2,8] For this reason, the temperatures of the sulfuric acid and oxalic acid solutions were kept at 0°C and 15°C, respectively, by an ice-cold water bath. During anodization, the electrolyte (side **A**) and the distilled water (side **B**) were effectively stirred with magnetic stirring bars for the maintenance of a constant temperature. A platinum wire was used as a cathode. The cell voltage was controlled by a DC power supplier. 20 and 60 V were mainly used for the anodizations in sulfuric acid and in oxalic acid, respectively. The film thickness can be fairly accurately predicted by a theoretically determined formation rate of the barrier layer, calculated at a current density 10 mA/cm^2, of 0.3 μm/min.[8,18] It was found in all cases that the thickness obtained was almost the same as the predicted value. This suggests that pore widening might be minimized under the conditions described above.

After ca. 50 μm films had been yielded on the aluminum substrate, they were throughly rinsed with distilled water. The back side (side **B**) of the aluminum substrate, attached with an o-ring smaller than that on the front side, was etched by a 20 wt% HCl, 0.1 M $CuCl_2$ solution at room temperature until the aluminum metal was just removed. Although water and hydrogen permeabilities had been preliminarily examined for a membrane with the barrier layer, no detectable flux was observed even when a rather high pressure of 10^7 Pa was applied. This indicates that even a fairly small molecule such as hydrogen cannot permeate the thin barrier layer and that the layer must be removed for the preparation of membranes.

To remove the barrier layer, side **B** of the cell was filled with a 20% H_2SO_4 solution for membranes prepared in sulfuric acid (abbreviated S-membrane). Because the thickness of the barrier layer (ca. 60 nm) of membranes formed in oxalic acid (abbreviated O-membranes) at 60 V was much thicker than that of the S-membranes (ca. 20 nm), the etchant used was a 4% phosphoric acid solution instead of the sulfuric acid. About 40 to 50 minutes were required for removal of the barrier layers of both the membranes. Side **A** was filled with a 1 M acetate buffer solution with a hydrostatic pressure of 30 cm-aqua in order to protect the porous layer. After the etching of the barrier layers, the membranes with peripheral aluminum were washed with water and dried in a vacuum.

It was necessary to remove the peripheral aluminum for a high-temperature experiment because of the thermal stress formed at the interface between the aluminum and the oxide layer. For this purpose, a bromine-methanol or a mercuric chloride solution was used.[22]

1.2 Apparatus for gas permeation and ultrafiltration

A schematic diagram of the gas permeability measurement apparatus is shown in **Fig. 3**. The membrane (effective area; 3.14 cm^2) was mounted in a diffusion cell in which the peripheral aluminum was used for sealing. The gas was fed into the high-pressure side of the cell after it had been evacuated by a rotary pump (<0.1 Pa) for 2 hs. The flux of the permeated gas was measured by a soap-film flowmeter. Pressure differences of less than 10^5 Pa were measured by a mercury manometer. The temperature of the cell was controlled by air, liquid nitrogen and methanol-dry ice baths.

The ultrafiltration equipment used was a Toyo Roshi-UHP-25 for aqueous solutions and an all-

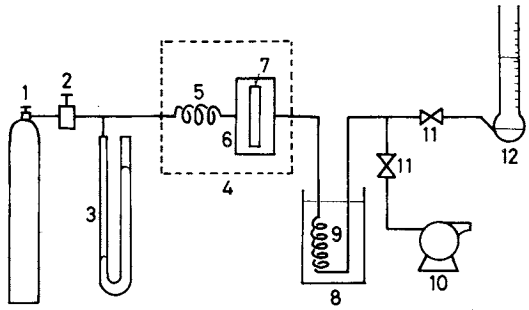

Fig. 3. Schematic diagram of apparatus for gas flow measurements. 1) gas cylinder; 2) pressure regulator; 3) mercury manometer; 4, 8) temperature baths; 5, 9) coils for preheating and cooling; 6) diffusion cell; 7) membrane; 10) vacuum pump; 11) vent valves; 12) soap-film flow-meter.

Pyrex cell with a stirring bar for organic solutions. The solutions were rigorously stirred in order to minimize concentration polarization.[7] The temperature was kept at 20°C by a water bath. Nearly monodispersed polyethylene glycols (PEG) (M_w: 2000, 4000, 7500, 18,000, 39,000 and 150,000) and polystyrenes (PS) (M_w: 946, 2800, 5200, 10,300 and 42,800) were used for ultrafiltration experiments with the aqueous and benzene solutions, respectively. Solutions of vitamin-B_{12} (M_w: 1,355), bovine serum-hemoglobin (M_w: 64,000), -alubumin (M_w: 67,000) and -γ-globulins (M_w: 150,000) were also examined. The concentration of the solutions was adjusted to 1.0 g/l in all cases. The concentrations of various solutes were determined by a total organic carbon analyzer (Toshiba-Beckman-915) and gel permeation chromatography (Toyo Soda-HLC-802).

2. Results and Discussion

2.1 Membrane characterization

Figure 4 shows an example of the membranes prepared by the procedure described in the experimental section. The size of the membrane can be easily controlled by changing the size of the o-rings used. Films prepared in oxalic acids are yellow, while those prepared in sulfuric acids are almost completely transparent, as shown in Fig. 4.

The structure of the membranes was directly observed by a scanning electron microscope (SEM) (Hitachi-8010) with a 3 nm resolution. About 3 nm of Pt-Pd (20 wt%) was sputtered on the samples. **Figure 5** shows the SEM photographs of the cross sections of an S-membrane and an O-membrane. The membranes were photographed just after completion of the etching of aluminum. The photographs reveal several points. The diameters of the pores are about 10 nm and 20 nm for the S-membrane and the O-membrane, respectively. The barrier layers can be clearly seen at the top of the membranes, whose

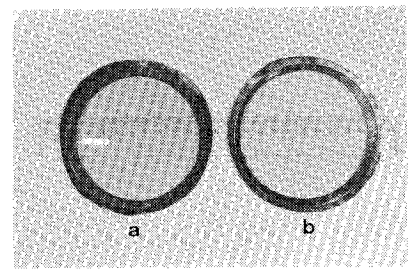

Fig. 4. Photographs of membranes. **a** and **b** are membranes prepared in sulfuric acid and in oxalic acid, respectively.

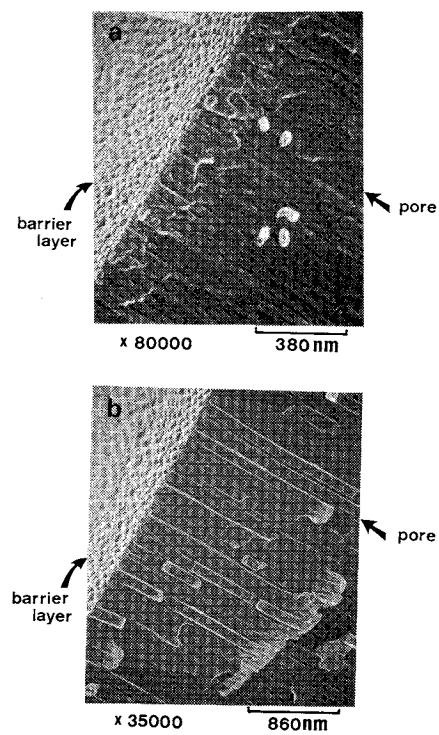

Fig. 5. SEM photographs of cross sections of membranes. **a** and **b** are for S-membrane and for O-membrane. Calibrating bars are 380 nm (**a**) and 860 nm (**b**), respectively.

thicknesses are ca. 20 nm and 60 nm for each. Single pores in each of the close-packed cells are formed perpendicularly to the macroscopic surface. Note that almost the same diameters were observed at the end of the pore, i.e. the side opposite to the barrier layer, suggesting the formation of pores with uniform diameters. It can also be seen in Fig. 5 that the distances between pores are ca. 50 nm and 140 nm for the S-membrane and the O-membrane, respectively. After etching of the barrier layer, it could easily be seen in SEM that all the pores went straight through the membrane.

It is noteworthy that a small-angle X-ray scattering technique has been applied in this study for the determination of the structure of the porous layer.[14] The observation indicated clearly that the dimensions of the hexagonally close-packed pores were almost the same and the pores were formed vertically to the

surface of the aluminum substrate as observed in SEM.

Table 1 represents a comparison of the film parameters for the S-membrane and the O-membrane. The results shown in Table 1 are in good agreement with those in the literature.[8)]

2.2 Ultrafiltration

2.2.1 Pure solvent permeability

The flux (J_v) of solvent through capillary tubes with uniform radius (r_0) may be expressed by the Hagen-Poiseuille equation:

$$J_v = \pi r_0^4 \cdot (P_1 - P_2) \cdot N / 8\eta l \qquad (1)$$

Where P_1, P_2, N, η and l are the pressures upstream and downstream, the areal density of the pore, the viscosity of the solvent and the membrane thickness, respectively. The fluxes of the various solvents were linearly increased by an increase in the pressure difference ($P_1 - P_2$). **Figure 6** shows the relationship of the fluxes of the pure solvents to the inversion of their viscosities ($1/\eta$) for an S-membrane with a film thickness of 65 μm. A straight line with an intercept of zero has been obtained, indicating that the flow of the solvents is basically expressed by the Hagen-Poiseuille equation as expected above. From the slope of the solid line in Fig. 6, the diameter of the pore is estimated as ca. 13 nm following the values of $l = 65\,\mu$m and $N = 4.6 \times 10^{10}/\text{cm}^2$. The areal density of the pore is calculated by an assumption that the distance between pores is 50 nm for the S-membranes. An identical experiment was carried out using an O-membrane, yielding a value of ca. 20 nm for the diameter. The above results point to an important feature of the anodic oxide membrane, namely that very few parameters are required for its characterization. This particular situation would be extremely important for the precise adaptation of the filter to the required permeation properties. The Nuclepore membrane is known to be a filter with rather precisely defined diameters and with pores which go straight through the membrane.[1,31)] The nuclear track technique applied for the Nuclepore membrane offers a variation in diameter of the pores in the range of a few hundred angstroms to a few hundred micrometers, controlled by the time of development.[25,31)] In the case of the anodic oxide membranes, it is also possible to control precisely the diameter of the pore by the etching procedure. When the membranes prepared here were immersed in sulfuric acid for a certain period of time, the fluxes of the solvents were increased, indicating that the walls of the pore were etched gradually. This circumstance is essentially the same for the Nuclepore membrane. Consequently, the anodic oxide membrane will be found to have a number of applications similar to those already found for the Nuclepore membrane.[19)]

Table 1. Dimensions of the membranes

		S-Membrane	O-Membrane
D	[nm]	50	140
$2r_0$	[nm]	10 ~ 12	~20
Porosity	[m²/g]	4.8	1.1
N[a)]	[cm⁻²]	4.6×10^{10}	5.9×10^{9}

[a)] The surface pore density.

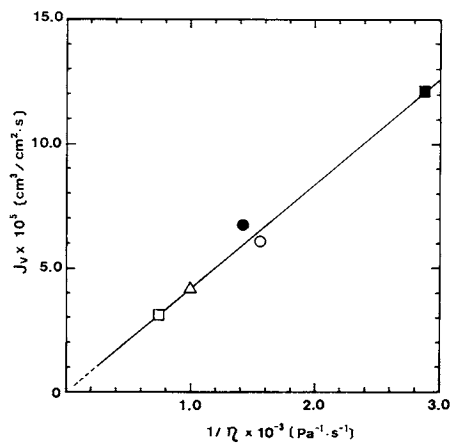

Fig. 6. Relationship of fluxes of pure solvents to inversion of viscosities. □, ethanol; △, water; ●, benzene; ○, methanol; ■, acetone ($P_1 - P_2 = 1.0 \times 10^5$ Pa).

The flux of the solvents themselves is fairly constant over several days except for water. In the case of the permeation of water, the flux generally decreases at a constant pressure. A typical result was that the flux of triply distilled water became half of the initial value after 5 hrs. However, it was found that this kind of behavior is strongly dependent on the concentration of proton (i.e. pH) of the water used. With water of pH = 3.3 adjusted by sulfuric acid, the decrease in flux was greatly suppressed. About 80% of the initial flux was observed after 24 hrs. These results may suggest that the initially formed aluminum oxide is changed to a hydrate form (böemite) under a condition. It is well known that the pores are fairly easily sealed in boiling water or steam, resulting in a drastic reduction of porosity.[3,8,33)] Although the actual mechanism for the decrease in the flux of water is still unclear in this study, it will be important for industrial applications of the anodic oxide films.

Applications of the usual polymeric membranes have been limited in aqueous solutions because of their poor resistance to organic solvents. There have been efforts to synthesize membranes having the solvent resistance such as a polyimide membrane.[15)] As stated above, the anodic oxide membrane showed a very stable permeation of organic solvents. This suggests potential utility for the ultrafiltration of synthetic polymer solutions.

2.2.2 Rejection of Polyethylene glycols, proteins and polystyrenes

Because of the decrease in the flux of water, measurement of the rejection of polyethylene glycols (PEG) was performed using freshly prepared membranes. Water permeability for each membrane was first measured and then the solution was filtered. The volume fluxes of various experiments were the same as those of pure solvents. No specific decrease in the fluxes has been observed, indicating that PEG and PS as well as the proteins used do not adsorb on the anodic oxide membranes whereas it is well known that polymers and proteins adsorb strongly on polymeric ultrafiltration membranes.[5,34]

Figure 7 shows the rejection for the S-membranes as a function of molecular weight. The observed rejection (R_{ob}) is defined as:

$$R_{ob}=1-\frac{C_p}{C_f} \tag{2}$$

where C_f and C_p are the concentrations of the bulk feed and product streams, respectively. The rejection was measured at a pressure difference ($P_1-P_2=1.0\times10^5$ Pa). For a theoretical treatment derived by Kedem and Katchalsky,[16,30] it is necessary to measure the dependence of the rejection on the volume flux[21,23] and to correct the observed rejection due to the concentration polarization.[19,24] However, the rejection characteristic shown in Fig. 7 clearly indicates that the molecular weight cut-off of the S-membrane was about 10,000 for both solutions. The molecular weight cut-off of the S-membrane seems reasonable in view of the "pore theory" in which the sizes of the solutes and of the pore are primarily important.[21,32,34] Note that the rejection characteristics shown in Fig. 7 seem to give a fairly sharp cut-off behavior. This might be due to the pore structures of uniform size and shape in the anodic oxide membranes.

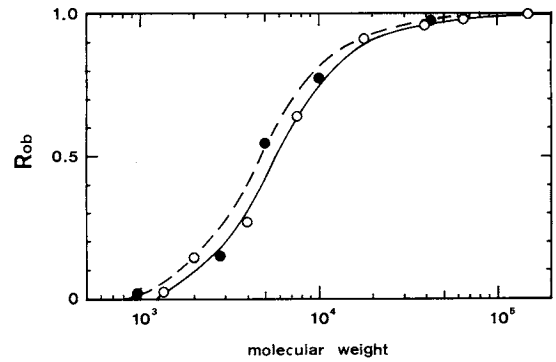

Fig. 7. Observed rejections of aqueous solutions of polyethylene glycols (PEG) and proteins and of benzene solutions of polystyrenes (PS) for S-membrane. —○—, aqueous solutions; ---●---, benzene solutions. PEG, M_w: 2000, 4000, 7500, 18,000, 39,000 and 150,000. Proteins, M_w: 1355, 64,000, 67,000, 150,000. PS, M_w: 946, 2800, 5200, 10,300, 42,800.

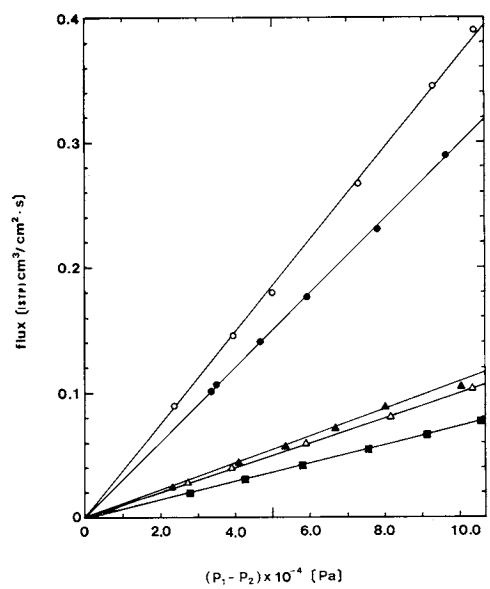

Fig. 8. Pressure dependence of fluxes of various gases at 290 K. ○, H_2; ●, He; △, N_2; ▲, CO; ■, CO_2.

2.3 Gas permeability

It has been usually considered that three flow mechanisms must be involved for permeability of gaseous molecules through a membrane with porous structures, i.e., Knudsen flow, viscous flow and surface diffusional flow (F_s). The total mole flux (F_t) may be expressed by the sum of the three terms,[11]

$$F_t=4\pi r_0^3\cdot(P_1-P_2)\cdot N\cdot\sqrt{2/\pi MRT}/3l + \pi r_0^4\cdot(P_1^2-P_2^2)\cdot N/16\eta_g lRT+F_s \tag{3}$$

where M and η_g are the molecular weight and the viscosity of the gas, respectively. There have been extensive studies on the permeability of gases through porous Vycor glass, demonstrating the significance of the surface flows.[11-13,26,27]

Figure 8 shows typical examples of the pressure dependence of the fluxes of various gases at a constant temperature. Upstream pressures could be increased up to 2×10^5 Pa. The observed fluxes were perfectly linear with the upstream pressure as shown in Fig. 8, indicating that the permeabilities were constant at a given temperature. No pressure effect has been observed in any case as long as the pressure difference was less than 10^5 Pa. This result strongly suggests that the flow of gases through anodic oxide membranes can be explained by Knudsen diffusion and surface diffusion only. Because the pore diameter is obviously less than the mean free path in this condition, viscous flow should be negligible.

To clarify the contribution of the surface flow,[12,26,27] the temperature dependence of the fluxes was examined. **Table 2** lists the permeability data of

Table 2. Permeability data for various gases at different temperatures[a)]

T [K]	H_2	He	N_2	CO_2	CO	C_2H_6	C_3H_8
77	—	4.7	—	—	—	—	—
195	4.4	5.0	4.3	—	4.7	4.9	—
290	4.4	4.9	4.6	4.1	5.0	4.2	4.1
322	4.7	5.4	4.6	4.3	—	—	—
370	4.9	5.1	4.5	4.3	—	—	—

[a)] $Q\sqrt{MT}\times 10^7$. Q and M are the permeability [(STP) $cm^3\cdot cm/cm^2\cdot s\cdot Pa$] and the molecular weight, respectively.

various gases (H_2, He, N_2, CO_2, CO, C_2H_6, C_3H_8) obtained at different temperatures. The permeability (Q) is defined as the flux at a pressure difference and at unit thickness of the membrane.[12] **Figure 9** shows the relation of $Q\sqrt{MT}$ vs. temperature. This figure indicates the permeability data for only He and CO_2 for the sake of clarity. The results are that the observed values of $Q\sqrt{MT}$ are about the same and no temperature dependence is found in any of the cases. These results strongly indicate that the flow of the gases used should be explained by the Knudsen regime alone. On the other hand, it has been previously reported that nitrogen, oxygen, carbon dioxide and even helium show surface flows in the Vycor system. In particular, carbon dioxide has a significant surface flow even at rather high temperatures.[12,27] The dashed line indicates the data for CO_2 reported by Hwang and Kammermeyer.[12] Shindo *et al.* have recently observed a similar effect.[27] However, the flow of carbon dioxide seems to be explained simply by the Knudsen regime in the present case. This crucial difference in the temperature dependences observed for anodic oxide membranes and for Vycor glass may be explained by the difference in specific surface areas of the two materials. The specific surface area of the Vycor glass previously examined is about $200\,m^2/g$.[12,27] On the other hand, the area of the S-membrane can be calculated as about $5\,m^2/g$ based on its structure, assuming that the density of the oxide is equal to $3.4\,g/cm^3$. The specific surface area of the anodic oxide membrane is two orders of magnitude less than that of the Vycor glass. The absence of surface flow seems to be due to this small specific surface area. The theoretical value of $Q\sqrt{MT}$ is calculated as 4.7×10^{-7} from the first term of Eq. (3), using the following values: $N=4.6\times 10^{10}\,cm^{-2}$, $r_0=5\,nm$ and $l=50\,\mu m$. Comparison of this theoretical value and the experimental one shows that the magnitude of the fluxes is also a predictable quantity, just as in the fluxes of pure solvents shown in Fig. 6. It is interesting to note that the permeability of the gases for anodic oxide membranes is about the same as that of Vycor glass,[12] even though the porosity of the

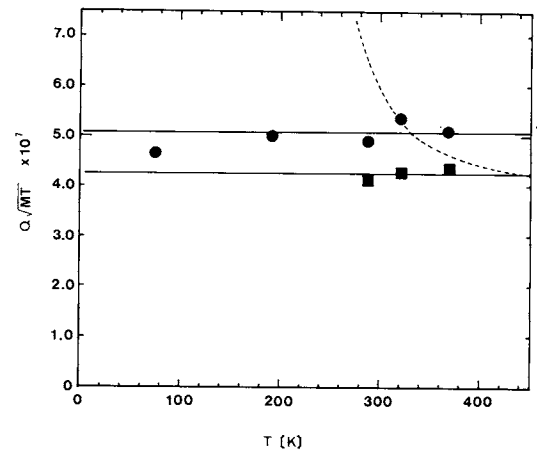

Fig. 9. Permeability data for He and CO_2 at different temperatures. ●, He; ■, CO_2. Dashed line indicates data for CO_2 reported by Hwang and Kammermeyer.[12]

anodic oxide membranes is considerably smaller. This may be due to the difference in the tortuosity of the pores, because the tortuosity in the anodic oxide membranes is essentially unity.

We have examined the O-membranes as well as the S-membranes prepared under various conditions of etching of the barrier layers changing the diameter of the pore. The fluxes were increased with increasing diameter of the pore in a way predicted by the Knudsen regime.

Finally, it must be pointed out that both S-membrane and O-membrane can be used at temperatures over 500°C. Membranes without the peripheral aluminum were prepared and then baked at 500°C for 2 hrs. After this thermal treatment, the permeability of the gases was remeasured. The values were almost exactly the same as those of the untreated membranes. This result suggests that anodic oxide membranes are useful for gas separations at high temperature.

Conclusion

The purpose of this study was to describe the preparation method and the basic nature of anodic aluminum oxide membranes. The flow of solvents through the membranes without a barrier layer was perfectly explained by the Hagen-Poiseuille equation. The membranes showed a strong resistance to organic solvents. The molecular weight cut-off was determined for membranes prepared in sulfuric acid, yielding values of ca. 10,000. The permeability of the gases was examined at different temperatures. The flow was explained by the Knudsen regime. No surface flow was observed. It is suggested that the membranes are useful for gas separations at high temperature.

Acknowledgment

We are most grateful to Professor N. Baba and Dr. K. Mizuki (Tokyo Metropolitan Univ.) for helpful discussions. Discussions

with Professor I. Uchida were very helpful. We thank Mr. T. Shimizu for helping with the experiments and Toyo Soda Company for polymer samples.

Nomenclature

$C_{p,f}$	=	concentration of solute	[mol/cm^3]
D	=	oxide cell size	[cm]
$F_{t,s}$	=	gas flow rate	[mol/cm^2·s]
J_v	=	solvent flow rate	[cm^3/cm^2·s]
l	=	membrane thickness	[cm]
M	=	molecular weight	[g/mol]
N	=	areal pore density	[/cm^2]
$P_{1,2}$	=	pressure	[Pa]
Q	=	gas permeability	[(STP)cm^3·cm/cm^2·s·Pa]
R_{ob}	=	observed rejection	[—]
R	=	gas constant	[J/K·mol]
r_0	=	radius of pore	[cm]
T	=	absolute temperature	[K]
η	=	viscosity of solvent	[Pa·s]
η_g	=	viscosity of gas	[Pa·s]

Literature Cited

1) Altug, I. and M. L. Hair: *J. Phys. Chem.*, **72**, 599 (1968).
2) Baba, N.: "Handbook of Aluminum Surface Treatment," Chapter 4, Light Metal Publishing Co. (1980).
3) Baker, B. R. and R. M. Pearson: *J. Electrochem. Soc.*, **119**, 160 (1972).
4) Ballou, E. V., T. Wydeven and M. I. Leban: *Env. Sci. and Techn.*, **5**, 1032 (1971).
5) Bauser, H., H. Chmiel, N. Stroh and E. Walitza: *J. Membrane Sci.*, **11**, 321 (1982).
6) Belfort, G. and J. Scherfig: *Desalination*, **18**, 43 (1976).
7) Colton, C. K., S. Friedman, D. E. Wilson and R. S. Lees: *J. Clin. Inv.*, **51**, 2472 (1972).
8) Diggle, J. W., T. C. Downie and C. W. Goulding: *Chem. Rev.*, **69**, 365 (1969).
9) Findlay, A.: "Osmotic Pressure," Longmans, London (1913).
10) Havredaki, V. and J. H. Petropoulos: *J. Membrane Sci.*, **12**, 303 (1983).
11) Huckins, H. E. and K. Kammermeyer: *Chem. Eng. Progr.*, **49**, 180 (1953).
12) Hwang, S. T. and K. Kammermeyer: *Can. J. Chem. Eng.*, **44**, 82 (1966).
13) Hwang, S. T. and K. Kammermeyer: *Separ. Sci.*, **2**, 555 (1967).
14) Itaya, K., K. Arai, S. Saito, Y. Takakuwa, N. Miyamoto and Y. Siota: to be published.
15) Iwama, A. and Y. Kazuse: *J. Membrane Sci.*, **11**, 297 (1982).
16) Kedem, O. and A. Katchalsky: *Biochim. Biophys. Acta*, **27**, 229 (1959).
17) Keller, F., M. S. Hunter and D. L. Robinson: *J. Electrochem. Soc.*, **100**, 411 (1953).
18) Liechti, F. and W. D. Treadwell: *Helv. Chem. Acta*, **30**, 1204 (1947).
19) Lonsdale, H. K.: *J. Membrane Sci.*, **10**, 81 (1982).
20) Nagayama, M. and K. Tamura: *Electrochimica Acta*, **12**, 1097 (1967).
21) Nakao, S. and S. Kimura: *J. Chem. Eng. Japan*, **14**, 32 (1981).
22) O'Sullivan, J. P. and G. C. Wood: *Proc. Roy. Soc. London, Ser. A*, **317**, 511 (1970).
23) Peppas, N. P. and D. L. Meadows: *J. Membrane Sci.*, **16**, 361 (1983).
24) Porter, M. C.: *Ind. Eng. Chem. Prod. Res. Develop.*, **11**, 234 (1972).
25) Riedel, C. and R. Spohr: *Ber. Bunsenges. Phys. Chem.*, **83**, 1165 (1979).
26) Sandler, S. I.: *Ind. Eng. Chem. Fundam.*, **11**, 424 (1972).
27) Shindo, Y., T. Hakuta, H. Yoshitome and H. Inoue: *J. Chem. Eng. Japan*, **16**, 120 (1983).
28) Shor, A. J., K. A. Kraus, W. T. Smith, Jr. and J. S. Johnson, Jr.: *J. Phys. Chem.*, **72**, 2200 (1968).
29) Smith, A. W.: *J. Electrochem. Soc.*, **120**, 1068 (1973).
30) Spiegler, K. S. and O. Kedem: *J. Gen. Physiol.*, **45**, 143 (1961).
31) Spohr, R.: *J. Electrochem. Soc.*, **128**, 188 (1981).
32) Verniory, A., R. Du Bois, P. Decsodt, J. P. Gassee and P. P. Lambert: *J. Gen. Physiol.*, **62**, 489 (1973).
33) Wood, G. C. and J. P. O'Sullivan: *J. Electrochem. Soc.*, **116**, 1351 (1969).
34) Zeman, L. J.: *J. Membrane Sci.*, **15**, 213 (1983).